Mist Cannon Trucks Can Exacerbate Secondary Organic Aerosol Formation and $PM_{2.5}$ Pollution in the Road Environment

Yu Xu[1], Xin-Ni Dong[2], Chen He[3], Dai-She Wu[4], Hong-Wei Xiao[1], Hua-Yun Xiao[1,*]

[1]School of Environmental Science and Engineering, Shanghai Jiao Tong University, Shanghai 200240, China

[2]Jiangxi Province Science and Technology Information Institute, Nanchang 330000, China

[3]State Key Laboratory of Heavy Oil Processing, China University of Petroleum, Beijing 102249, China

[4]School of Resource, Environmental and Chemical Engineering, Nanchang University, Nanchang 330031, China

*Corresponding author: Hua-Yun Xiao

E-mail: xiaohuayun@sjtu.edu.cn

Phone: +86-173-0183-7060

Table of Contents

Parameter Calculation and Compound Categorization.

The value of double-bond equivalent (DBE) was calculated to reflect the sum of π-bonds and rings in a neutral molecule (Lechtenfeld et al., 2014; Qiao et al., 2020). The equation was shown below.

$$DBE = 1 + N_C - N_H/2 + N_N/2 \quad (1)$$

where the N_C, N_H, and N_N denote the number of carbon, hydrogen, and nitrogen atoms in a molecular formula, respectively.

The modified aromaticity index (AI_{mod}) can be used to reflect the aromaticity of organic molecules, which was calculated by the following equation (Koch and Dittmar, 2006; Schmidt et al., 2017).

$$AI_{mod} = (1 + N_C - 0.5 \times N_O - N_S - 0.5 \times N_N - 0.5 \times N_H)/(N_C - 0.5 \times N_O - N_S - N_N) \quad (2)$$

where the N_C, N_H, N_O, N_N, and N_S denote the number of carbon, hydrogen, oxygen, nitrogen, and sulfur atoms in a molecular formula, respectively.

The carbon oxidation state (OSc) is an indicator to describe the evolving composition of aerosol organics undergoing oxidation processes (Kroll et al., 2011). For assignable molecular formulas, OS_C was calculated with following equation.

$$OS_C \approx 2 \times N_O/N_C - N_H/N_C \quad (3)$$

where the N_C, N_H, N_O, and N_N denote the number of carbon, hydrogen, oxygen, and nitrogen atoms in a molecular formula, respectively. Although the heteroatoms (N, S, and P) can introduce some uncertainties to the OS_C of a given molecule in the measurement of ultrahigh resolution ESI-MS, the influences of these heteroatoms on OS_C of the orgainc aerosols are generally small (Kroll et al., 2011).

In this sutdy, the molecular formulas of organic molecules were classified into five categories according to the AI_{mod} range and ratios of H/C and O/C. Specifically, these categories include (A) unsaturated aliphatic-like (1.5 ⩽ H/C < 2.0), (B) highly unsaturated-like (AI_{mod} ⩽ 0.5 and H/C < 1.5), (C) highly aromatic-like (0.5 < AI_{mod} ⩽ 0.67), (D) polycyclic aromatic-like (AI_{mod} > 0.67), and (E) saturated-like (H/C ⩾ 2.0 or O/C ⩾ 0.8) molecules (Seidel et al., 2014; Sihui et al., 2021). Considering that the numerous isomers of each formula, the divided categories only represent the compounds cantaining the most likely functional structure mentioned above (Butturini et al., 2020; Xie et al., 2021).

Aerosol Liquid Water (ALW) Prediction

The model ISORROPIA-II was used to estimate the water mass concentration with particle-phase concentrations of Na^+, NH_4^+, K^+, Ca^{2+}, Mg^{2+}, SO_4^{2-}, NO_3^-, and Cl^-, as well as meteorological data (ambient temperature and relative humidity) as inputs (Guo et al., 2015; Nguyen et al., 2016; Tan et al., 2017). In this study, the model was run in the “reverse mode” without inputs of gas-phase parameters (Nguyen et al., 2015; Xu et al., 2020). In addition, the thermodynamically metastable state was set in the subsequent calculation (Guo et al., 2015; Nguyen et al., 2015; Nguyen et al., 2016). The “forward mode” was also run with inputs of only particle-phase ion concentration data, temperature, and relative humidity. The calculation results of water concentrations showed little difference irrespective of the mode used, which is consistent with the previous measurements (Guo et al., 2015; Hennigan et al., 2015).

Due to the complex composition of aerosol organics, it is difficult to directly quantify the mass concentration of water associated with organic fraction (Cruz and Pandis, 2000; Nguyen et al., 2016; Sareen et al., 2013). Accordingly, the mass concentration of water derived from organic compounds was predicted using a simplified model with the Zdanovskii−Stokes−Robinson (ZSR) mixing rule, as suggested by previous studies (Nguyen et al., 2015; Nguyen et al., 2016). Briefly, the hygroscopic growth of aerosol mixtures can be estimated using weighted hygroscopicity of each component according to their dry volume fractions (Bian et al., 2014; Nguyen et al., 2014; Nguyen et al., 2016). The detailed calculation was shown below (Kreidenweis et al., 2008; Petters and Kreidenweis, 2007).

$$V_{w,o} = V_o \kappa_{org} a_w / (1 - a_w) \quad (4)$$

where $V_{w,o}$ and V_o are the volumes of water and organics, respectively. κ_{org} is dimensionless and represents the hygroscopicity parameter of the organics. a_w is also dimensionless and indicates water activity. The typical value of 1.4 g cm^{-3} for organic density was used to calculate the V_o value (Davidson et al., 2005; Turpin and Lim, 2001). In this study, the κ_{org} value of 0.08 was used for urban aerosol (Cerully et al., 2015; Dusek et al., 2010; Gunthe et al., 2009; Nguyen et al., 2016). The a_w value can be treated as relative humidity to simplify the calculation (Nguyen et al., 2015). This consideration was based on the following assumptions. The effect of aerosol curvature is insignificant. Furthermore, the effect of aerosol water uptake on ambient vapor pressure is also negligible (Bian et al., 2014). However, this assumption may lead to an overestimation in hygroscopicity (4–11%) (Nguyen et al., 2014).

Table S1. The arithmetic and peak-intensity-weighted averages of the elemental ratios and DBE values for different compound subgroups in different $PM_{2.5}$ samples.

	All compounds			CHO			CHON		
$PM_{2.5}$ samples	O/C ± SD O/C_w	H/C ± SD H/C_w	DBE ± SD DBE_w	O/C ± SD O/C_w	H/C ± SD H/C_w	DBE ± SD DBE_w	O/C ± SD O/C_w	H/C ± SD H/C_w	DBE ± SD DBE_w
Air spray	0.52 ± 0.21	1.35 ± 0.36	6.93 ± 3.33	0.46 ± 0.17	1.24 ± 0.35	7.61 ± 3.19	0.49 ± 0.19	1.21 ± 0.31	8.61 ± 3.17
(23 March)	0.56	1.56	4.51	0.49	1.27	7.04	0.46	1.24	8.22
Ground aspersion	0.53 ± 0.21	1.27 ± 0.41	7.44 ± 3.64	0.47 ± 0.17	1.09 ± 0.38	8.45 ± 3.52	0.47 ± 0.16	1.05 ± 0.31	9.79 ± 2.98
(23 March)	0.55	1.56	4.57	0.49	1.05	8.95	0.43	1.13	9.18
Air spray	0. 49± 0.2	1.33 ± 0.36	7.15 ± 3.32	0.44 ± 0.17	1.21 ± 0.36	8.06 ± 3.59	0.45 ± 0.17	1.20 ± 0.30	8.71 ± 2.73
(24 March)	0.52	1.56	4.58	0.47	1.23	7.57	0.42	1.24	8.28
Ground aspersion	0.55 ± 0.21	1.29 ± 0.40	7.30 ± 3.61	0. 48 ± 0.15	1.08 ± 0.38	9.50 ± 4.13	0.50 ± 0.16	1.07 ± 0.31	9.40 ± 2.79
(24 March)	0.57	1.57	4.45	0.50	1.06	9.21	0.47	1.14	8.88
Air spray	0.46 ± 0.19	1.23 ± 0.41	8.36 ± 4.18	0.42 ± 0.15	1.09 ± 0.40	9.57 ± 4.38	0.42 ± 0.15	1.06 ± 0.33	10.47 ± 3.60
(25 March)	0.45	1.48	5.54	0.43	1.07	9.27	0.39	1.10	9.88
Ground aspersion	0.18 ± 0.21	1.25 ± 0.39	12.00 ± 3.48	0.49 ± 0.17	1.14 ± 0.38	7.68 ± 3.18	0.49 ± 0.16	1.07 ± 0.31	9.66 ± 3.10
(25 March)	0.57	1.59	4.23	0.52	1.10	8.07	0.46	1.15	8.88
No water spray (A)	0.55 ± 0.22	1.29 ± 0.38	7.49 ± 3.69	0.47 ± 0.16	1.14 ± 0.36	8.96 ± 4.14	0.51 ± 0.17	1.09 ± 0.31	9.44 ± 2.97
(26 March)	0.54	1.54	4.79	0.50	1.14	8.54	0.45	1.14	8.97
No water spray (B)	0.52 ± 0.21	1.31 ± 0.38	7.18. ± 3.37	0.47 ± 0.17	1.18 ± 0.36	8.07 ± 3.45	0.48 ± 0.16	1.10 ± 0.31	9.27 ± 2.88
(26 March)	0.61	1.56	4.47	0.49	1.17	8.09	0.47	1.15	8.83

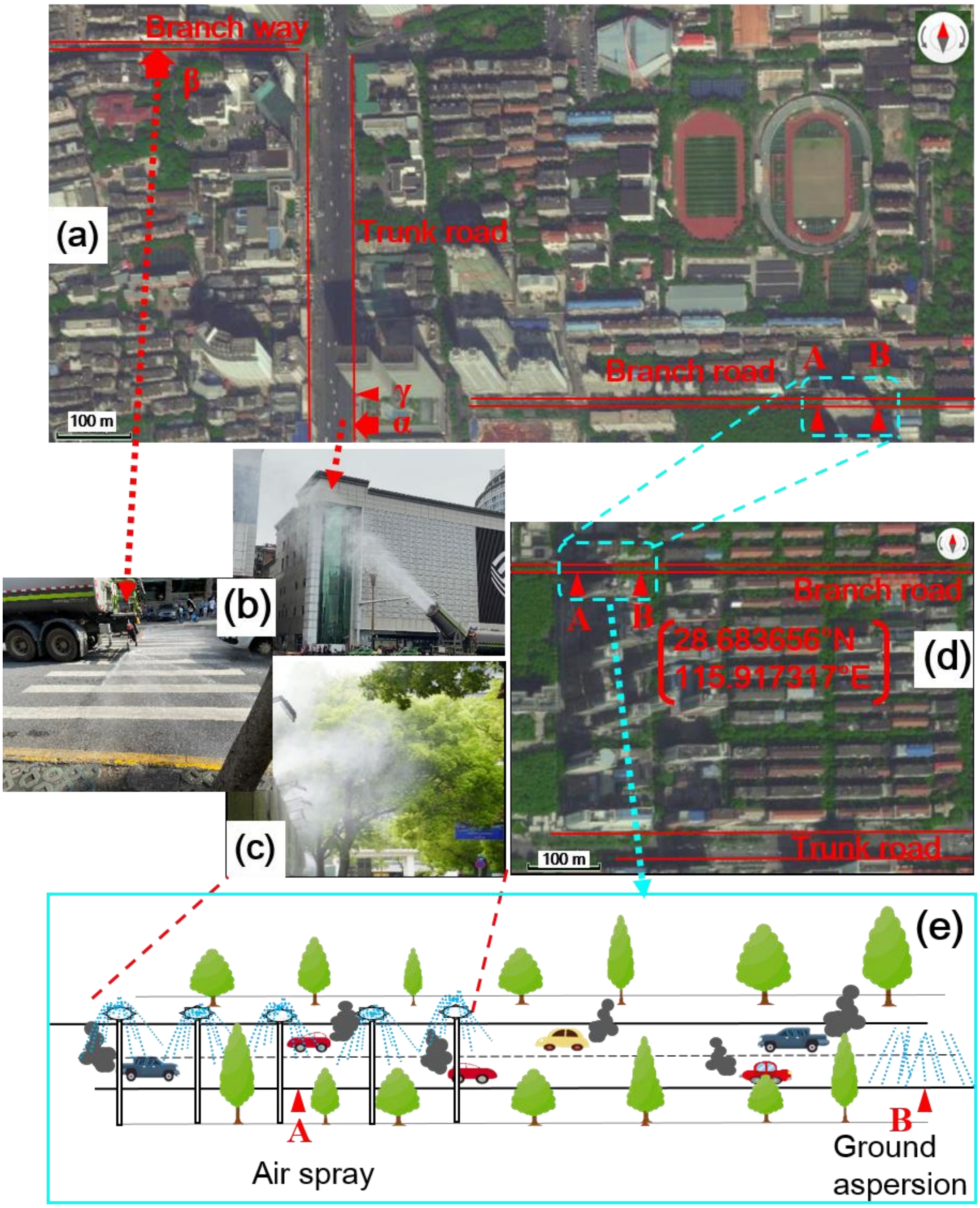

Figure S1. Map and diagram showing (a) the location and surrounding of the sampling site. The symbol of "γ" indicates the location where $PM_{2.5}$ mass concentration was monitored before and after mist cannon truck passed. The symbols of "α" and "β" refer to (b) the locations where the mist cannon truck photograph and the traditional sprinkling truck photograph were taken respectively. The symbol of "A" indicates that (d) the sampling was conducted on the air spray road segment or no water spray road segment (A). The symbol of "B" indicates that (d) the sampling was conducted on the ground aspersion road segment or no water spray road segment (B). The conceptual diagram of the sampling campaign is shown in figure (e). The maps (figure a and d) are from the Baidu map (Baidu, China).

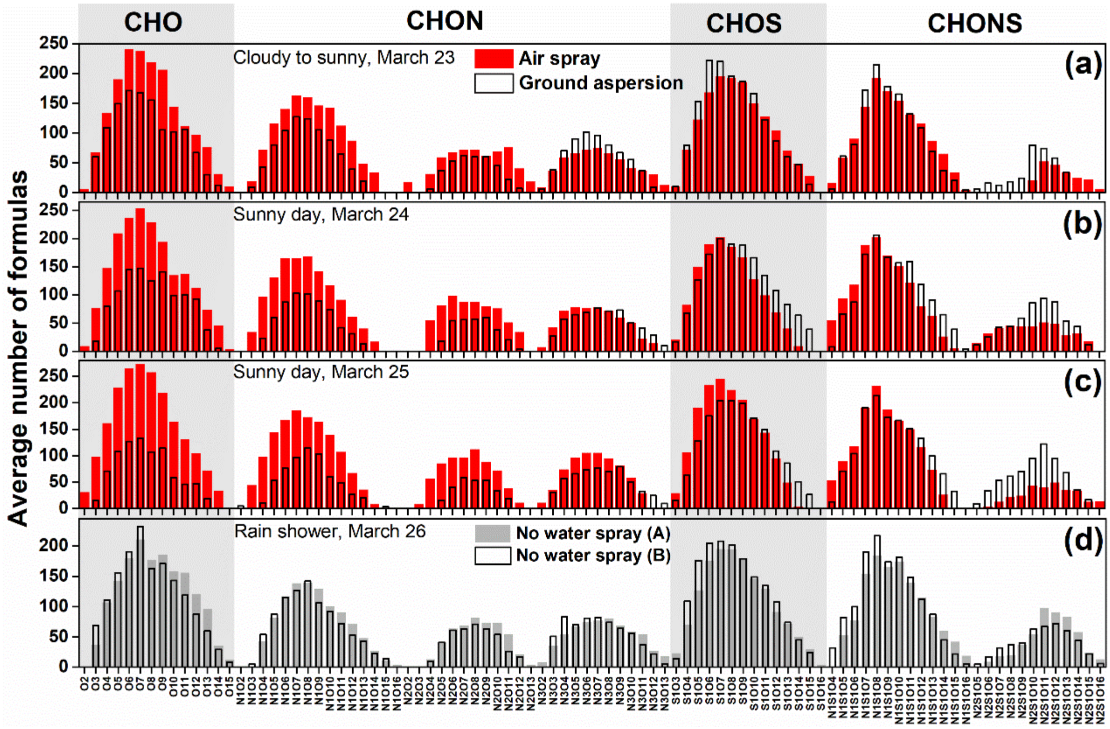

Figure S2. Classification of CHO, CHON, CHOS, and CHONS species into subgroups according to the number of O atoms in their molecules in WSOM in $PM_{2.5}$ collected from different cases: (a, b, and c) air spray road segment vs ground aspersion road segment and (d) no water spray road segment (A) vs no water spray road segment (B).

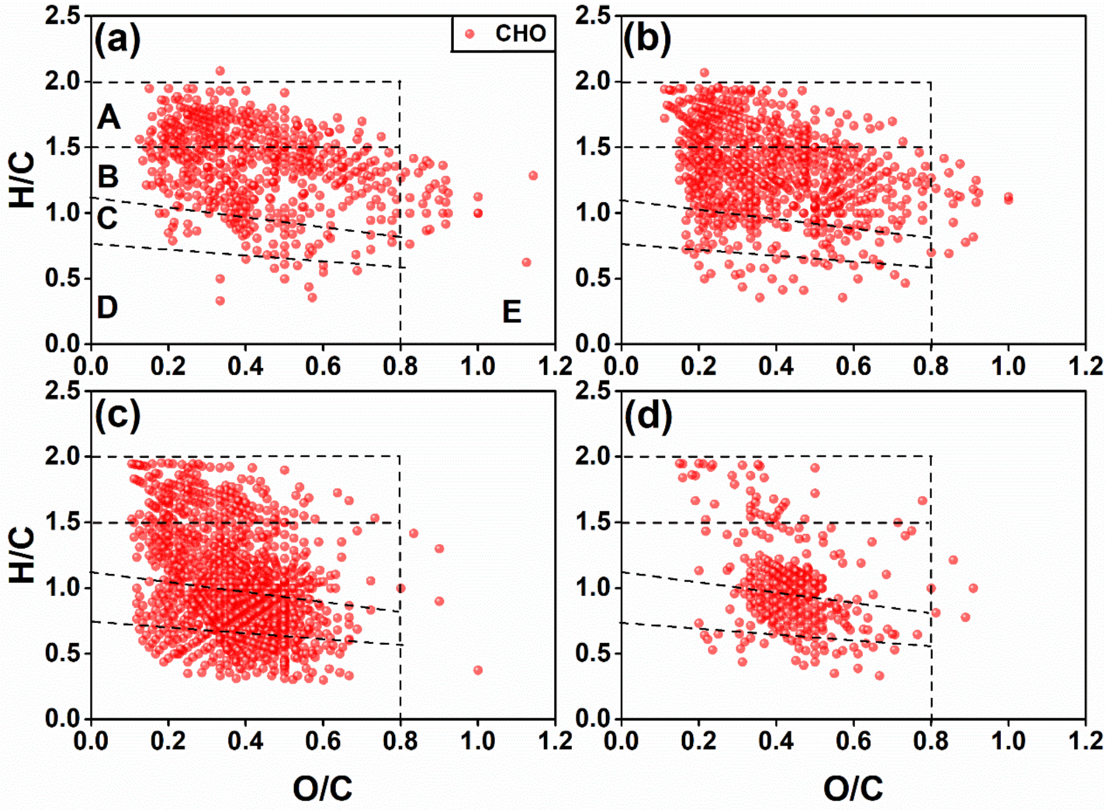

Figure S3. Van Krevelen diagrams of unique CHO compounds in WSOM in $PM_{2.5}$ collected from different cases: air spray road segment vs ground aspersion road segment on (a) March 23, (b) March 24, and (c) March 25 and two road segments without water spray (A vs B) on (d) March 26. For the above cases of paired comparison, the unique CHO compounds indicate the CHO molecules identified in $PM_{2.5}$ collected from the air spray (/no water spray-A) road segments. The classifications of compounds include (A) unsaturated aliphatic-like, (B) highly unsaturated-like, (C) highly aromatic-like, (D) polycyclic aromatic-like, and (E) saturated-like molecules.

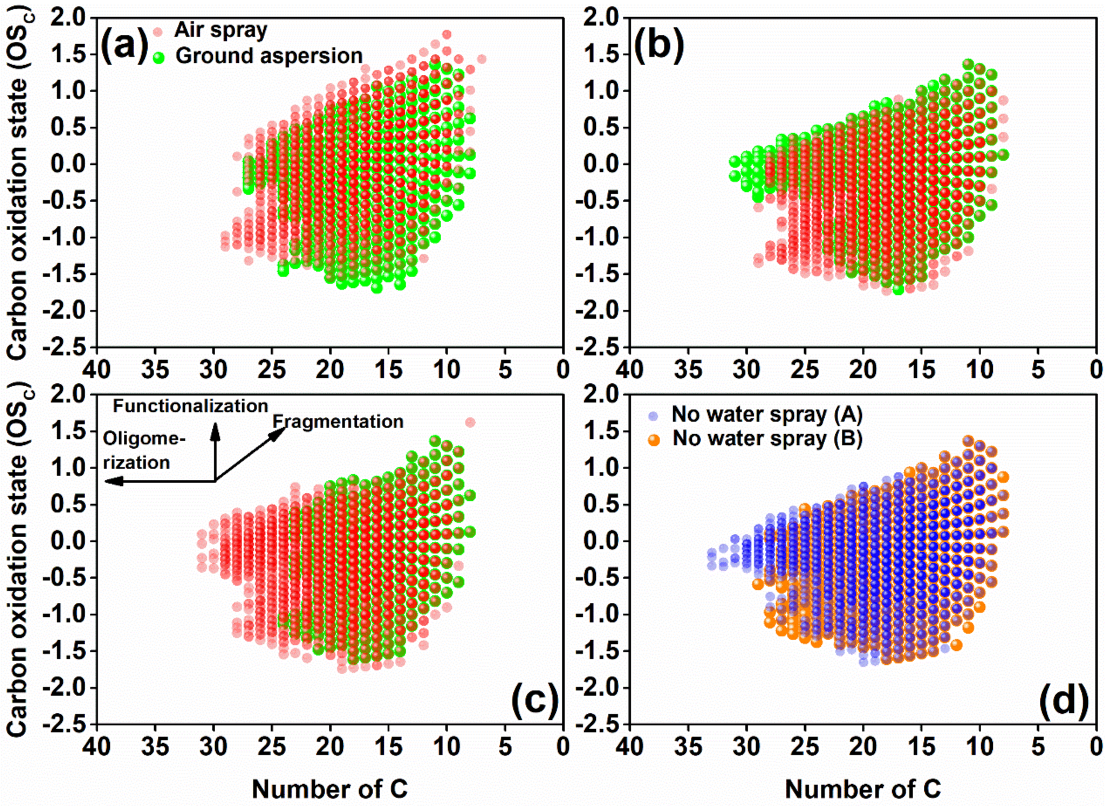

Figure S4. OS_c of each CHO molecule in WSOM in $PM_{2.5}$ collected from different cases: air spray road segment vs ground aspersion road segment on (a) March 23, (b) March 24, and (c) March 25 and no water spray road segment (A) vs no water spray road segment (B) on (d) March 26.

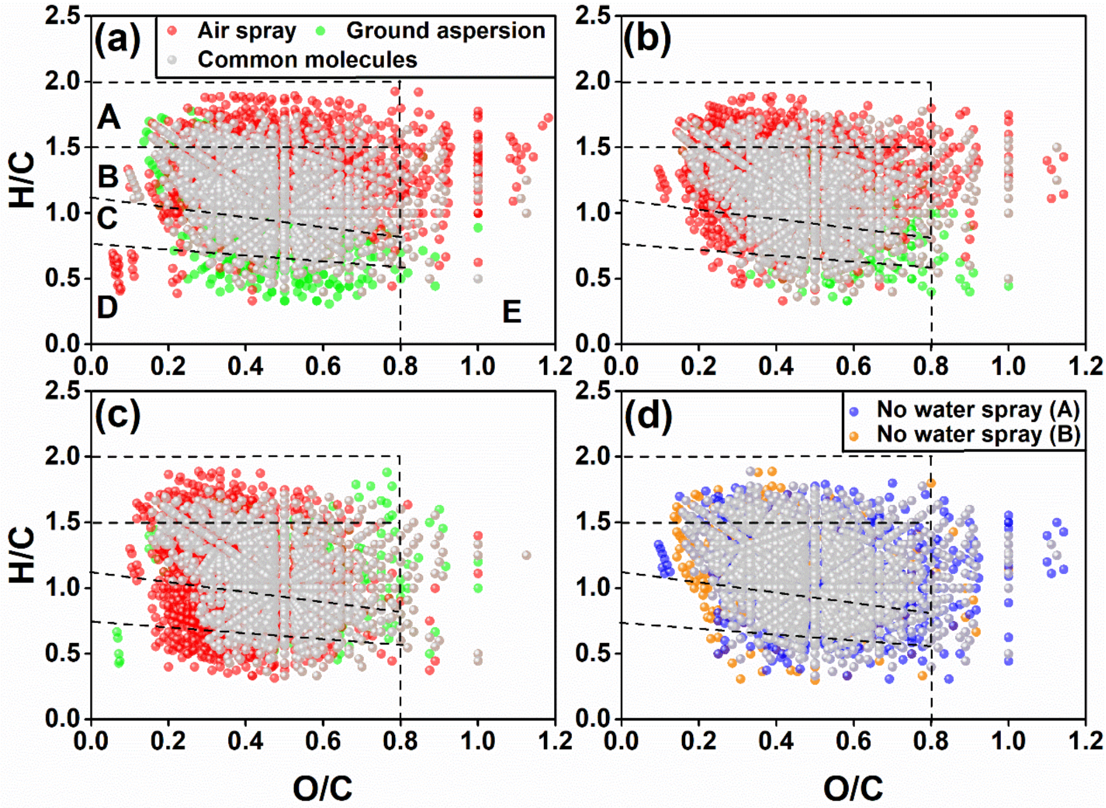

Figure S5. Van Krevelen diagrams of CHON compounds in WSOM in $PM_{2.5}$ collected from different cases: air spray road segment vs ground aspersion road segment on (a) March 23, (b) March 24, and (c) March 25 and two road segments without water spray (A vs B) on (d) March 26. The circles of different colors indicate the unique organic compounds identified in the above cases of paired comparison. Common molecules identified in different cases are shown as gray circles. The classifications of compounds include (A) unsaturated aliphatic-like, (B) highly unsaturated-like, (C) highly aromatic-like, (D) polycyclic aromatic-like, and (E) saturated-like molecules.

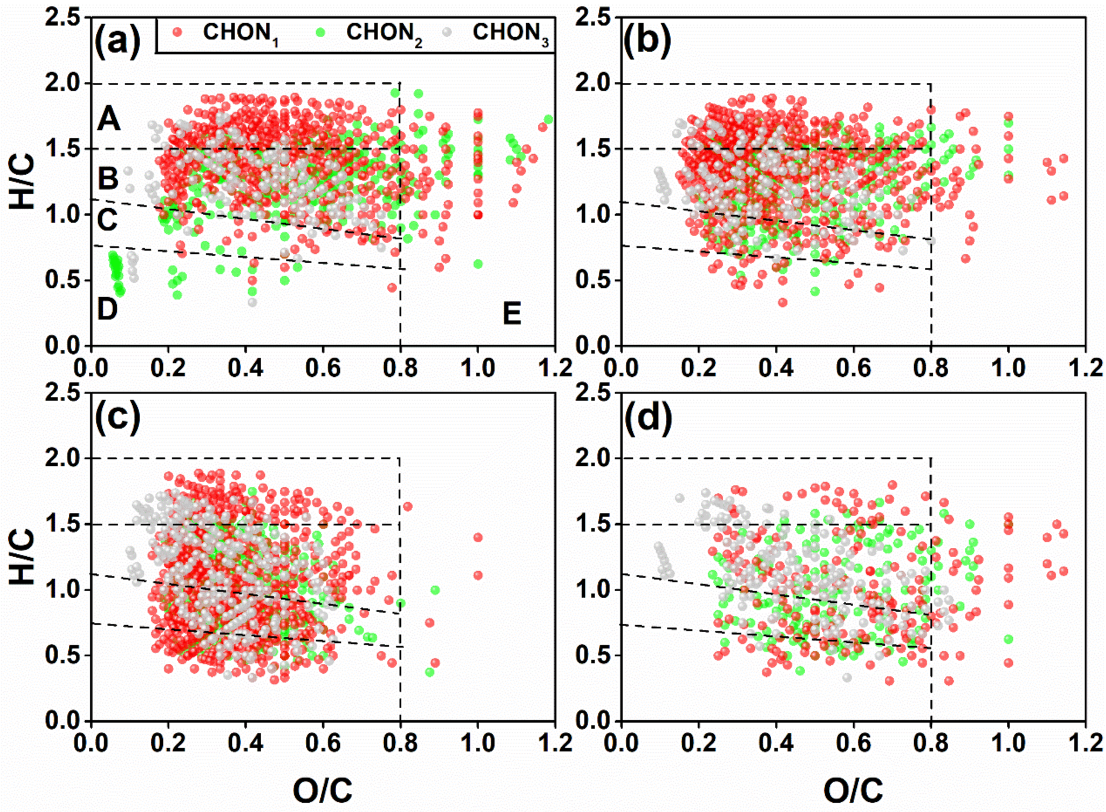

Figure S6. Van Krevelen diagrams of unique CHON compounds in WSOM in PM2.5 collected from different cases: air spray road segment vs ground aspersion road segment on (a) March 23, (b) March 24, and (c) March 25 and two road segments without water spray (A vs B) on (d) March 26. For the above cases of paired comparison, the unique CHON compounds indicate the CHON molecules identified in $PM_{2.5}$ collected from the air spray (/no water spray-A) road segments. The classifications of compounds include (A) unsaturated aliphatic-like, (B) highly unsaturated-like, (C) highly aromatic-like, (D) polycyclic aromatic-like, and (E) saturated-like molecules.

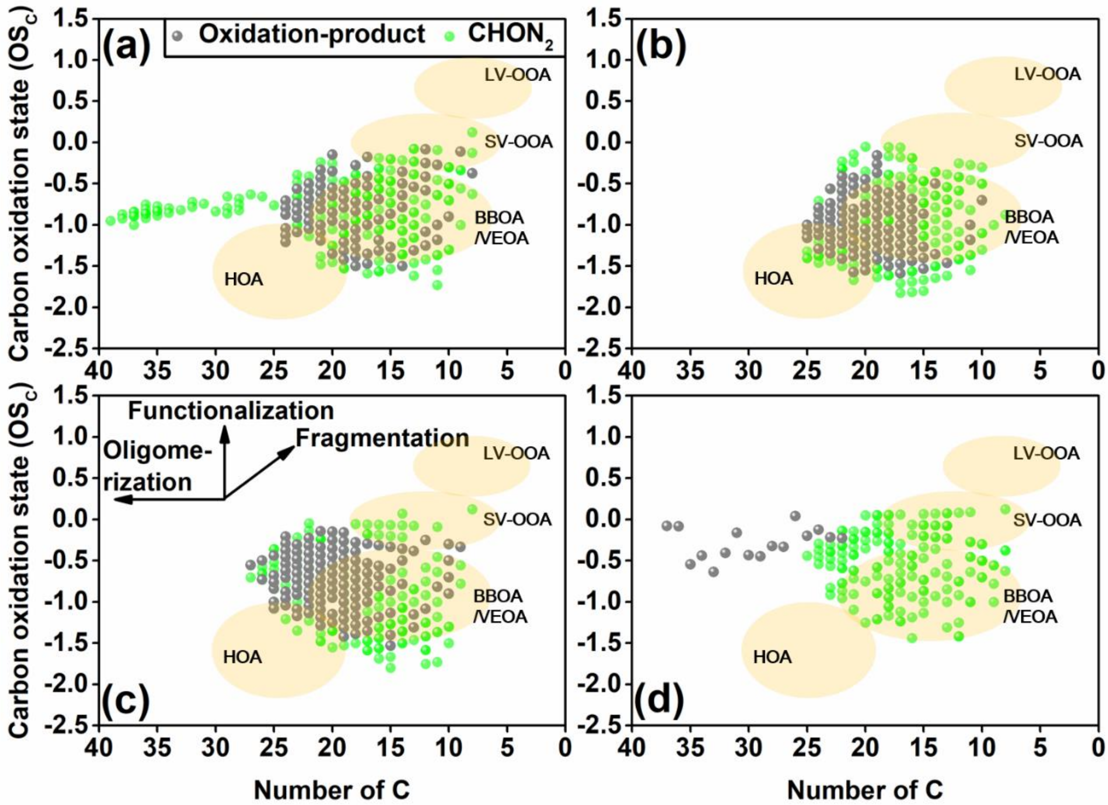

Figure S7. OS_c of unique $CHON_2$ molecules in WSOM in $PM_{2.5}$ collected from different cases: air spray road segment vs ground aspersion road segment on (a) March 23, (b) March 24, and (c) March 25 and two road segments without water spray (A vs B) on (d) March 26. For the above cases of paired comparison, the unique $CHON_2$ compounds indicate the $CHON_2$ molecules identified in $PM_{2.5}$ collected from the air spray (/no water spray-A) road segments. The light orange background indicates areas of HOA (hydrocarbon-like organic aerosol), BBOA and VEOA (biomass burning and vehicle emission organic aerosols) (Kroll et al., 2011; Tong et al., 2016), SV-OOA (semivolatile oxidized organic aerosol), and LV-OOA (low-volatility oxidized organic aerosol) (Kroll et al., 2011). The grey circles refer to the identified oxidation-product pairs.

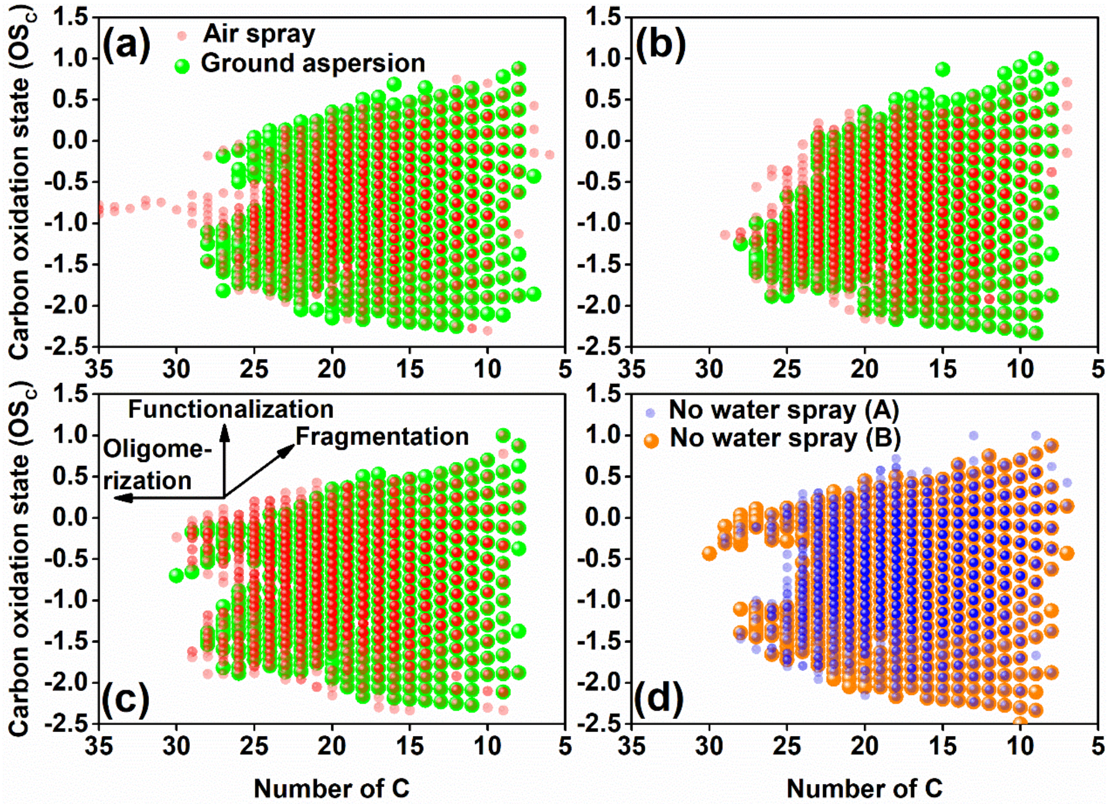

Figure S8. OS_c of each CHON molecule in WSOM in $PM_{2.5}$ collected from different cases: air spray road segment vs ground aspersion road segment on (a) March 23, (b) March 24, and (c) March 25 and no water spray road segment (A) vs no water spray road segment (B) on (d) March 26.

References

Bian, Y., Zhao, C., Ma, N., Chen, J., Xu, W.: A study of aerosol liquid water content based on hygroscopicity measurements at high relative humidity in the North China Plain, Atmos. Chem. Phys., 14(12): 6417-6426, 2014.

Butturini, A., Herzsprung, P., Lechtenfeld, O. J., Venturi, S., Amalfitano, S., Vazquez, E., Pacini, N., Harper, D. M., Tassi, F., Fazi, S.: Dissolved organic matter in a tropical saline-alkaline lake of the East African Rift Valley, Water Res., 173: 115532, 2020.

Cerully, K., Bougiatioti, A., Hite Jr, J., Guo, H., Xu, L., Ng, N., Weber, R., Nenes, A.: On the link between hygroscopicity, volatility, and oxidation state of ambient and water-soluble aerosols in the southeastern United States, Atmos. Chem. Phys., 15(15): 8679-8694, 2015.

Cruz, C. N., Pandis, S. N.: Deliquescence and hygroscopic growth of mixed inorganic−organic atmospheric aerosol, Environ. Sci. Technol., 34(20): 4313-4319, 2000.

Davidson, C. I., Phalen, R. F., Solomon, P. A.: Airborne Particulate Matter and Human Health: A Review, Aerosol Sci. Technol., 39(8): 737-749, 2005.

Dusek, U., Frank, G., Curtius, J., Drewnick, F., Schneider, J., Kürten, A., Rose, D., Andreae, M. O., Borrmann, S., Pöschl, U.: Enhanced organic mass fraction and decreased hygroscopicity of cloud condensation nuclei (CCN) during new particle formation events, Geophys. Res. Lett., 37: 3, 2010.

Gunthe, S., King, S., Rose, D., Chen, Q., Roldin, P., Farmer, D., Jimenez, J., Artaxo, P., Andreae, M., Martin, S.: Cloud condensation nuclei in pristine tropical rainforest air of Amazonia: size-resolved measurements and modeling of atmospheric aerosol composition and CCN activity, Atmos. Chem. Phys., 9(19): 7551-7575, 2009.

Guo, H. Y., Xu, L., Bougiatioti, A., Cerully, K. M., Capps, S. L., Hite Jr, J., Carlton, A., Lee, S. H., Bergin, M., Ng, N.: Fine-particle water and pH in the southeastern United States, Atmos. Chem. Phys., 15(9): 5211-5228, 2015.

Hennigan, C., Izumi, J., Sullivan, A., Weber, R., Nenes, A.: A critical evaluation of proxy methods used to estimate the acidity of atmospheric particles, Atmos. Chem. Phys., 15(5): 2775-2790, 2015.

Koch, B. P., Dittmar, T.: From mass to structure: an aromaticity index for high-resolution mass data of natural organic matter, Rapid Commun. Mass Spectrom., 20(5): 926-932, 2006.

Kreidenweis, S., Petters, M., DeMott, P.: Single-parameter estimates of aerosol water content, Environ. Res. Lett., 3(3): 035002. DOI: 10.1088/1748-9326/3/3/035002, 2008.

Kroll, J. H., Donahue, N. M., Jimenez, J. L., Kessler, S. H., Canagaratna, M. R., Wilson, K. R., Altieri, K. E., Mazzoleni, L. R., Wozniak, A. S., Bluhm, H., Mysak, E. R., Smith, J. D., Kolb, C. E., Worsnop, D. R.: Carbon oxidation state as a metric for describing the chemistry of atmospheric organic aerosol, Nat. Chem., 3(2): 133-139, 2011.

Lechtenfeld, O. J., Kattner, G., Flerus, R., Mccallister, S. L., Schmitt-Kopplin, P., Koch, B. P.: Molecular transformation and degradation of refractory dissolved organic matter in the Atlantic and Southern Ocean, Geochim. Cosmochim. Ac., 126: 321-337, 2014.

Nguyen, T. K. V., Capps, S. L., Carlton, A. G.: Decreasing Aerosol Water Is Consistent with OC Trends in the Southeast U.S, Environ. Sci. Technol., 49(13): 7843-7850, 2015.

Nguyen, T. K. V., Petters, M., Suda, S., Guo, H., Weber, R., Carlton, A.: Trends in particle-phase liquid water during the Southern Oxidant and Aerosol Study, Atmos. Chem. Phys., 14(20): 10911-10930, 2014.

Nguyen, T. K. V., Zhang, Q., Jimenez, J. L., Pike, M., Carlton, A. G.: Liquid water: ubiquitous contributor to aerosol mass, Environ. Sci. Tech. Let., 3(7): 257-263, 2016.

Petters, M., Kreidenweis, S.: A single parameter representation of hygroscopic growth and cloud condensation nucleus activity, Atmos. Chem. Phys., 7(8): 1961-1971, 2007.

Qiao, W., Guo, H., He, C., Shi, Q., Xiu, W., Zhao, B.: Molecular Evidence of Arsenic Mobility Linked to Biodegradable Organic Matter, Environ. Sci. Technol., 54(12): 7280-7290, 2020.

Sareen, N., Schwier, A., Lathem, T., Nenes, A., McNeill, V. F.: Surfactants from the gas phase may promote cloud droplet formation, P. Natl. Acad. Sci. U. S. A., 110: 2723-2728, 2013.

Schmidt, F., Koch, B. P., Goldhammer, T., Elvert, M., Witt, M., Lin, Y.-S., Wendt, J., Zabel, M., Heuer, V. B., Hinrichs, K.-U.: Unraveling signatures of biogeochemical processes and the depositional setting in the molecular composition of pore water DOM across different marine environments, Geochim. Cosmochim. Ac., 207: 57-80, 2017.

Seidel, M., Beck, M., Riedel, T., Waska, H., Suryaputra, I. G. N. A., Schnetger, B., Niggemann, J., Simon, M., Dittmar, T.: Biogeochemistry of dissolved organic matter in an anoxic intertidal creek bank, Geochim. Cosmochim. Ac., 140: 418-434, 2014.

Sihui, S., Xie, Q., Lang, Y., Cao, D., Xu, Y., Chen, J., Chen, S., Hu, W., Qi, Y., Pan, X., Sun, Y., Wang, Z., Liu, C.-Q., Jiang, G., Fu, P.: High Molecular Diversity of Organic Nitrogen in Urban Snow in North China, Environ. Sci. Technol., 2021.

Tan, H., Cai, M., Fan, Q., Liu, L., Li, F., Chan, P. W., Deng, X., Wu, D.: An analysis of aerosol liquid water content and related impact factors in Pearl River Delta, Sci. Total Environ., 579: 1822-1830, 2017.

Tong, H., Kourtchev, I., Pant, P., Keyte, I., O'Connor, I. P., Wenger, J., Pope, F., Harrison, R., Kalberer, M.: Molecular composition of organic aerosols at urban background and road tunnel sites using ultra-high resolution mass spectrometry, Faraday Discuss., 189: 51-68, 2016.

Turpin, B. J., Lim, H.-J.: Species Contributions to PM2.5 Mass Concentrations: Revisiting Common Assumptions for Estimating Organic Mass, Aerosol Sci. Technol., 35(1): 602-610. DOI: 10.1080/02786820119445, 2001.

Xie, Q., Sihui, S., Chen, J., Dai, Y., Yue, S., Su, H., Tong, H., Zhao, W., Ren, L., Xu, Y., Cao, D., Li, Y., Sun, Y., Wang, Z., Liu, C.-Q., Kawamura, K., Jiang, G., Cheng, Y., Fu, P.: Increase of nitrooxy organosulfates in firework-related urban aerosols during Chinese New Year's Eve, Atmos. Chem. Phys., 21: 11453-11465, 2021.

Xu, Y., Miyazaki, Y., Tachibana, E., Sato, K., Ramasamy, S., Mochizuki, T., Sadanaga, Y., Nakashima, Y., Sakamoto, Y., Matsuda, K., Kajii, Y.: Aerosol Liquid Water Promotes the Formation of Water-Soluble Organic Nitrogen in Submicrometer Aerosols in a Suburban Forest, Environ. Sci. Technol., 54(3): 1406-1414, 2020.